Published in final edited form as:
Menopause. 2011 June ; 18(6): 698–708. doi:10.1097/gme.0b013e31820390a2.

nNOS Inhibition Improves Diastolic Function and Reduces Oxidative Stress in Ovariectomized-mRen2.Lewis Rats

Jewell A. Jessup, BS[1], **Lili Zhang, MD**[2], **Alex F. Chen, MD, PhD**[2], **Tennille D. Presley, PhD**[3,4,*], **Daniel B. Kim-Shapiro, PhD**[3,4], **Mark Chappell, PhD**[5], **Hao Wang, MD, PhD**[6], and **Leanne Groban, MD**[1,6]

[1] Department of Physiology and Pharmacology, Wake Forest University School of Medicine, Winston Salem, North Carolina

[2] Department of Surgery, University of Pittsburgh School of Medicine, and Vascular Surgery Research, Veterans Affairs Pittsburgh Healthcare System, Pittsburgh, Pennsylvania

[3] Department of Physics, Wake Forest University, Winston-Salem, North Carolina

[4] Translational Science Center, Wake Forest University, Winston-Salem, North Carolina

[5] Hypertension and Vascular Research Center, Wake Forest University School of Medicine, Winston-Salem, North Carolina, USA

[6] Department of Anesthesiology, Wake Forest University School of Medicine, Winston-Salem, North Carolina, USA

Abstract

Objective—The loss of estrogen in mRen2.Lewis rats leads to an exacerbation of diastolic dysfunction. Since specific neuronal nitric oxide synthase inhibition reverses renal damage in the same model, we assessed the effects of inhibiting neuronal nitric oxide on diastolic function, left ventricular remodeling, and the components of the cardiac nitric oxide system in ovariectomized and sham-operated mRen2.Lewis rats treated with L-VNIO (0.5 mg/kg/day for 28 days) or vehicle (saline).

Methods—Female mRen2.Lewis rats underwent either bilateral oophorectomy (OVX; n=15) or sham-operation (Sham; n=19) at 4 weeks of age. Beginning at 11 weeks of age, the rats were randomized to receive either L-VNIO or vehicle.

Results—The surgical loss of ovarian hormones, particularly estrogen, led to exacerbated hypertension, impaired myocardial relaxation, diminished diastolic compliance, increased perivascular fibrosis, and increased relative wall thickness. The cardiac tetrahydrobiopterin (BH4)-to-dihydrobiopterin (BH2) levels were lower among OVX rats compared to sham-operated rats and this altered cardiac biopterin profile was associated with enhanced myocardial superoxide production and decreased nitric oxide release. LVNIO decreased myocardial reactive oxygen species production, increased nitrite concentrations, attenuated cardiac remodeling and improved diastolic function.

Conclusions—Impaired relaxation, diastolic stiffness and cardiac remodeling were found among OVX mRen2.Lewis rats. A possible mechanism for this unfavorable cardiac phenotype may have resulted from a deficiency in available BH4 and subsequent increase in nNOS-derived

Address correspondence to: Leanne Groban, MD, Department of Anesthesiology, Wake Forest University School of Medicine, Medical Center Boulevard, Winston Salem, NC 27157-1009, Phone: 336-716-4498, Fax: 336-716-8190, lgroban@wfubmc.edu.
*Dr. Tennille's current affiliation is Chemistry Department, Winston-Salem State University, Winston-Salem, NC.

Financial disclosure/conflicts of interest: None reported.

superoxide and reduction in NO metabolites within the heart. Selective nNOS inhibition with L-VNIO attenuated cardiac superoxide production and limited remodeling, leading to improved diastolic function in OVX mRen2.Lewis rats.

Keywords

diastolic function; fibrosis; left ventricular modeling; myocardial relaxation; nitric oxide; postmenopausal

Introduction

Research directed to explore the underlying mechanisms associated with the development and progression of heart failure is an important area of investigation as the incidence of this disease is reaching epidemic proportions.[1] Recent data of lengthened survival in male heart failure patients have not shown comparable benefits in women.[2,3] This is partly because research conducted to-date, as well as current treatment approaches, target systolic dysfunction, the more common type of heart failure in men as opposed to diastolic dysfunction in women. In fact, some estimates claim that 75% of diastolic heart disease patients are women over the age of 65.[4,5] The prognosis for these women is severe as there is a significant increase in hospitalizations compared to systolic heart failure patients,[1,6] and women with diastolic heart disease yield deaths rates greater than 20%.[7,8]

The mechanisms underlying diastolic dysfunction, the precursor of heart failure with normal ejection fraction or diastolic heart failure, are poorly understood, particularly in older women. The loss of estrogen following menopause has been linked to the development of hypertension and left ventricular hypertrophy;[9,10] two risk factors for diastolic dysfunction.[11] However, estrogen replacement therapy remains controversial given that data from the Women's Health Initiative have not shown protective cardiovascular benefits in postmenopausal women receiving estrogen therapy.[12] Additionally, the precise mechanism by which estrogen acts in females to offer cardioprotection is not completely clear though data demonstrates that estrogen modulates the production of nitric oxide (NO).[13–15] A role of the NO system in the progression of heart failure in postmenopausal women may be related to estradiol upregulation of endothelial nitric oxide synthase (eNOS) by stimulation of serine/threonine protein kinase Akt (protein kinase B).[16] The actions of eNOS as well as neuronal NOS (nNOS) have profound impacts on diastolic function by affecting nitric oxide bioavailability.[17] Furthermore, dysregulation of the NOS system may contribute to diastolic dysfunction based on several lines of evidence, including: a) regulated production of nNOS by estrogen;[18–21] and b)-the observation that estrogen receptor beta (ERs) mediates increases in cardiomyocyte eNOS levels.[22]

Surgical depletion of endogenous estrogen in experimental models results in significant changes in blood pressure and cardiovascular function. In our prior study, the development of diastolic dysfunction, interstitial fibrosis, and increased serum aldosterone was accelerated in female hypertensive mRen2.Lewis following oophorectomy.[23] The mRen2.Lewis strain, which expresses the mouse renin 2 (mRen2) gene in various tissues, is a congenic model of angiotensin II-dependent hypertension produced by the successive backcross of the (mRen-2)27 transgenic rat onto the Lewis background.[24] The female mRen2.Lewis is an estrogen-sensitive model since ovariectomy significantly exacerbates the degree of hypertension and estrogen replacement normalizes the blood pressure.[25] This model emulates the syndrome exhibited clinically in postmenopausal women.

Interestingly, in estrogen-depleted mRen2.Lewis rats, Yamaleyeva et al. reported that the renal expression of endothelial nitric oxide synthase (eNOS) was attenuated while neuronal

NOS (nNOS) content was increased.[26] Subsequent treatment with the selective nNOS inhibitor L-VNIO partially reversed the effects of oophorectomy on high blood pressure in the female mRen2.Lewis.[26] These authors speculated that L-VNIO may inhibit uncoupled nNOS to reduce the formation of superoxide resulting in a reduction in blood pressure. With this in mind, the current study was designed to investigate the hypothesis that suppression of the protective cardiac eNOS isoform with a concomitant reduction in nitric oxide production and/or an increase in the presumed deleterious nNOS isoform contributes to LV remodeling in the ovariectomized mRen2.Lewis rats. In addition, we evaluated whether the shift in the cardiac nNOS pathway from an adaptive (NO-producing NOS) to a maladaptive NOS [reactive oxygen species (ROS)-producing] is attenuated by the nNOS inhibitor.

Methods

Experimental Model

Experiments were conducted in congenic female mRen2.Lewis rats obtained from the transgenic rat colony of the Hypertension and Vascular Research Center of Wake Forest University School of Medicine. All experimental procedures were approved by the Animal Care and Use Committee of Wake Forest University. Rats were weaned at 3 wk of age and allowed to acclimate in a temperature-controlled, Association for Assessment and Accreditation of Laboratory Animal-approved facility (12-hr light/dark cycle) with free access to rat chow and tap water. At 4 wk of age, rats were randomly assigned to undergo either bilateral oophorectomy (OVX; n=15) or sham-operation (Sham; n=19) performed under 2% isoflurane anesthesia, as previously described.[23] At age 11 wk, the groups were further randomly divided to receive the specific nNOS inhibitor, N5-(1-Imino-3-butenyl)-l-ornithine (L-VNIO, Enzo Life Sciences International, Inc., Plymouth Meeting, PA) diluted in saline for a targeted dose of 0.5 mg/kg/day or pure saline as a vehicle control (VEH) both delivered intraperitoneally via an osmotic minipump (Model 2ML4, 2.5 μL/hr, 4 wk) [Sham +VEH n=9; Sham+L-VNIO n=10; OVX+VEH n=6; OVX+L-VNIO n=9].[26] Systolic blood pressure was monitored once weekly via tail-cuff plethysmography (NIBP-LE5001, Panlab, Barcelona, Spain) beginning with a training phase at 5 wk of age and continued through the termination of the study at 15 wk of age. Serum estradiol was measured at the completion of the study to verify complete oophorectomy and confirm depletion of circulating estrogen with a minimal detection limit of 5 pg/mL [Polymedco (Cortlandt Manor, NY)].

Echocardiographic evaluation

At 15 wk of age, cardiac dimensions and function were assessed in anesthetized (ketamine/xylazine: 80/12 mg/kg) animals using a Philips 5500 echocardiograph (Philips Medical Systems, Andover, MA) and a 12 MHz phased array probe as previously described.[23] LV mass was calculated using a standard cube formula, which assumes a spherical LV geometry according to the formula: LV mass (LVmass) = 1.04 × [[LVEDD + PWT + AWT]3 − LVEDD], where 1.04 is the specific gravity of muscle. Relative wall thickness (RWT) was calculated as: 2 × PWT/LVEDD.

Morphometry and Histopathology

Cardiac cross-sections, 2-mm thick, were fixed for 24 h in 4% paraformaldehyde followed by dehydration in graded ethanols before being embedded into paraffin blocks. Slices (4-μm) were mounted onto Superfrost Plus slides and stained with hematoxylin and eosin in order to measure myocyte cross-sectional area. Approximately 100 cardiomyocytes from 2 sections per rat were analyzed at 400× magnification using a Leica DM4000B microscope (Bannockburn, IL) with a tandem Leica DFC digital camera and Simple PCI 6.0 software. Additional slides were stained with Picrosirius red (PSR) to evaluate interstitial and perivascular collagen deposition within the tissue using polarized dark-field microscopy

[Olympus polarizing microscope system (Center Valley, PA) equipped with a Digital SPOT RT, 3-pass capture, thermoelectrically cooled charge-coupled camera (Sterling Heights, MI) and SPOT® Advanced software] as previously described.[27] Adobe Photoshop Creative Suite 3 (Adobe Inc., San Jose, CA) was used to determine the ratios of collagen positive stained pixels to unstained pixels in each photomicrograph (4 randomized quadrant field images per rat, magnified 200-times).

In situ ROS production

In situ production of reactive oxygen species (ROS) was determined using dihydroethidium (DHE), which reacts with O_2^- yielding the fluorescent product, 2-hydroxyethidium. Slices (3 sections per rat) were cut from frozen cardiac cross-sections and mounted in slides. The sections were then incubated with 10 μM DHE (Invitrogen Molecular Probes, Carlsbad, CA) in a humidified, light-protected chamber for 30 min at 37°C and then the nuclei counterstained with 4′,6-diamindino-2-phenylindole (DAPI, 30 μg/mL, Sigma-Aldrich, St. Louis, MO). Slides were the rinsed in PBS, cover slipped, and analyzed at 400× using a fluorescence microscope (Leica DM4000B, Bannockburn, IL; excitation = 510–550 nm, emission = 590 nm for DHE; excitation = 330–380 nm, emission 420 nm for DAPI) connected to a Leica DFC digital camera. The fluorescent signal intensities were analyzed within the heart using Simple PCI 6.0 software. All data are presented as average gray scale intensities ± SEM.

Western blot hybridization

Cardiac microsomes were prepared and protein concentrations were determined as previously reported.[23] Fifty micrograms of homogenate proteins were separated by SDS PAGE on a 7.5% acrylamide gel and transferred to a polyvinylidene fluoride membrane (PVDF, Bio-Rad, Hercules, CA). Immunocomplexes were detected with an anti-nNOS (1:2000), anti-eNOS (1:500), anti-phospho eNOS (1:1000) (BD Transduction Laboratories, Franklin Lakes, NJ), anti-sarcoplasmic calcium (SERCA) 2 ATPase (1:1000 dilution; Abcam, Cambridge, MA), anti-PLB (1:2000; Millipore, Temecula, CA), and anti-phospho-PLB Ser16 (1:5000; Millipore, Temecula, CA). To normalize the variability of protein loading, the antibody to elongation factor 1α (EF1α, 1:10,000 dilution, Millipore, Temecula, CA) or glyceraldehyde-3-phosphtate (GAPDH, 1:5000 dilution; Cell Signaling, Danvers, MA) was used as a loading control. The bound antibodies were resolved with a Super Signal West Pico chemiluminescent/enhancer kit (Pierce ECL Western Blotting Substrate, Pierce, Rockford, IL, USA), exposed to Amersham Hyperfilm (Amersham Biosciences, Piscataway, NJ), and analyzed using densitometry. The resulting densities were corrected for background and expressed as arbitrary units normalized to the EF1α intensities. Human endothelial cell lysate (eNOS) and rat cerebrum cell lysate (nNOS) were used as positive controls (BD Transduction Laboratories, Franklin Lakes, NJ).

Measurement of total biopterin and BH4 levels

The biopterin profile of the cardiac tissue was measured by HPLC with fluorescence detection as previously documented.[28] The cardiac supernatant was subjected to protein assay and BH4 detection. Protein was removed from supernatant by adding 10 μL of a 1:1 mixture of 1.5 M $HClO_4$ and 2 M H_3PO_4 to 90 μL of extracts, followed by centrifugation. Total biopterin (BH4, dihydrobiopterin [BH2] and oxidized biopterin [B]) was determined by acid oxidation whereby 10 μL of 1% iodine and 2% KI in 1 M HCl solution were added to 90 μL protein-free supernatant. BH2 plus B was determined by alkali oxidation by the addition of 10 μL of 1 M NaOH to 80 μL of the supernatant, followed by 10 μL of 1% iodine and 2% KI in 1 M NaOH solution. The acid-oxidation samples were protected from light and incubated for 1 hr at room temperature. Five microliters of fresh ascorbic acid (20 mg/mL) was then added to samples to reduce iodine, and 20 μL of 1 M H3PO4 was added to

acidify alkaline-oxidation samples prior to the ascorbic acid. The samples were centrifuged and 90 μL of the supernatant was injected into a 250-mm long, 4.6-mm inner diameter Spherisorb ODS-1 column (5 μm particle size; Alltech Associates, Inc., Deerfield, IL) isocratically eluted with a methanol-water (5:95, v/v) mobile phase running at a flow rate of 1.0 mL/min. Fluorescence (350 nm excitation, 450 nm emission) was detected by a fluorescence detector (RF10AXL, Shimadzu Co., Columbia, MD). BH4 concentration was calculated by subtracting BH2 and B from total biopterins.

Nitrite Measurements

Nitrite levels were measured using a chemiluminescence-based Nitric Oxide Analyzer (Sievers, Inc., GE Analytical Instruments, Boulder, CO). Nitrite is reduced in a sample chamber to release nitric oxide, which then goes to a reaction chamber where it reacts with ozone to form a quasi-stable chemiluminescent species. The sample chamber contains sodium iodide in glacial acetic acid to reduce the nitrite. The amount of light detected on a photodiode is proportional to the amount of released NO and hence nitrite in the sample. The integral of the voltage recorded is proportional to the detected light. The values observed in this study are typical of these measurements.[29] In addition to variation due to sample handling and instrumentation, nitrite is influenced mostly by NOS function, but also by diet. [29] Overall, the variability is small. For all measurements, standard curves were obtained and used for quantitative measurements.

Statistical analysis

All values are expressed as mean ± SEM. For serial blood pressure measurements, a 2 × 2 × 2 × 5 multivariate analysis of variance (MANOVA) was conducted to determine the relationship among the four groups and the changes in blood pressure over the duration of the experiment. The differences in the blood pressure levels were modeled as interactions between procedure (Sham vs. OVX); treatment (VEH vs. L-VNIO); before and after treatment; and time. The one 4-way factorial analysis and the three 3-way analyses indicated significant interactions among all the factors, which lead to further characterization of the differences after treatment commenced using one-way analyses of variance and Bonferroni post-*hoc* tests for each time point. For all other endpoints, two-way ANOVA evaluated significant effects of estrogen or L-VNIO. Significant interactions between the groups were further characterized using Bonferroni post-*hoc* tests. Analyses were performed using GraphPad Prism 5 (GraphPad, San Diego, CA) or SPSS (SPSS, Inc., Chicago, IL). Differences were considered significant at $p < 0.05$.

Results

Removal of the ovaries was associated with an increase in body weight, independent of nNOS inhibition (Table 1). Body weight in sham rats were not affected by treatment with L-VNIO. Estrogen depletion was confirmed by serum estradiol levels of <5 pg/mL and 27 ± 1.6 pg/mL in OVX- and sham-treated mRen2.Lewis rats, respectively. Heart weight was increased in estrogen-deficient rats compared to intact, but this can be attributed to the increased body size of the OVX-rats given that HW/BW were similar (Table 1), as reported previously.[23]

Progressive increases in systolic blood pressure (SBP) occurred in estrogen-intact and OVX-mRen2.Lewis rats from 5 to 11 wks (Figure 1). Similar to earlier findings,[25] substantial rises in blood pressure were observed by week 7 in OVX-rats as compared to intact littermates ($P < 0.0001$). This exacerbated hypertension continued throughout the duration of the 15-wk study [$\lambda (4,26) = 0.13$, $P < 0.0001$]. Commencement of chronic L-VNIO treatment led to modest reductions in systolic blood pressure in both intact and OVX rats g [$\lambda (1,29) = 0.58$,

P <0.0001]; however, the blood pressure lowering effects of L-VNIO- were not sustained in the estrogen-intact group (P > 0.05)

The effects of estrogen and nNOS inhibition on echocardiographic-derived variables indicative of systolic and diastolic function are summarized in Table 2 and Figure 2. Estrogen deficiency had no effect on M-mode measurements of LV chamber dimensions or systolic function, as signified by the absence of changes in %FS. Assessment of diastolic function using Doppler flow and Doppler tissue imaging showed impairment in diastolic function in estrogen-deplete mRen2.Lewis as demonstrated by a 22% decrease in mitral annular descent (e′) in OVX rats despite there being no effect on systolic function (Figure 2). Furthermore, the E/A ratio tended to be blunted in estrogen-deficient rats compared to sham-operated littermates as estrogen accounted for 9% percent of the variance in E/A [Estrogen: $F(1,33) = 3.18$, $P = 0.08$]. Treatment with L-VNIO offered preservation of myocardial function as reflected in a 21% reduction in filling pressure, combined with a positive effect on myocardial relaxation represented as the ratio of early to late mitral annular velocity (e′/a′; P =0.04; Table 2).

The reduction in myocardial relaxation in the OVX-mRen2.Lewis rats was not associated with changes in protein levels of SERCA2 or phospholamban, key proteins in cytosolic Ca^{2+} reuptake to the sarcoplasmic reticulum. Furthermore, the phosphorylation level of phospholamban was not altered by the removal of the ovaries or by L-VNIO (data not shown).

Although relative heart weights were similar among groups, estrogen and nNOS inhibition had notable effects on LV structure. There were increases in relative wall thickness in OVX-rats relative to intact rats (Estrogen effect: P<0.05). Administration of L-VNIO partially reversed the increased wall thickness [L-VNIO: $F(1,33) = 9.51$, $P = 0.004$] from significantly elevated values following OVX (Table 2). Moreover, ovariectomy in the mRen2.Lewis rats increased LV mass compared to intact littermates, and this remodeling effect was significantly attenuated by 4 wk of nNOS inhibition [L-VNIO: $F(1,33) = 4.65$, $P = 0.039$]. Importantly, these L-VNIO-mediated structural benefits were also observed in the estrogen-intact mRen2.Lewis rats, despite nominal changes in blood pressure.

Evaluation of LV hypertrophy following surgical estrogen depletion further showed that an increase in myocardial fibrosis was the primary trigger for remodeling rather than an increase in myocyte size. Perivascular collagen deposition was increased in OVX-rats compared with intact littermates (P=0.005), and this effect was improved by nNOS inhibition [L-VNIO effect: $F(1,100) = 51.91$, $P < 0.0001$] (Figure 3). While myocyte size was not altered by estrogen loss or L-VNIO (data not shown), dihydroethidium staining within myocytes revealed increased ROS generation in the OVX-mRen2.Lewis rats compared to intact littermates [Estrogen effect: $F(1,266) = 48.8$, $P < 0.0001$] (Figure 4). Importantly, the 4-wk administration of L-VNIO attenuated the DHE staining, particularly in OVX-rats [L-VNIO effect: $F(1,266) = 4.62$, $P = 0.0326$].

A potential explanation for enhanced ROS generation in the hearts from OVX-mRen2.Lewis rats is nNOS uncoupling, as estrogen influences the levels of tetrahydrobiopterin (BH4), an essential cofactor of nitric oxide synthase.[30,31] To examine the potential role of BH4 degradation as the limiting factor in NO versus ROS production, we measured the cardiac biopterin profile (B + BH2 +BH4). While there was no overall change in biopterin homeostasis in estrogen deficient rats, the balance between BH4 and BH2 was shifted such that the concentration of BH4 was decreased and BH2 increased (Figure 5). Specifically, estrogen accounted for 34% of the total variance in BH4 (P = 0.001), while simultaneously

increasing cardiac concentrations of BH2 [Estrogen: $F(1,25) = 6.36$, $P = 0.019$] (Figure 5). Specific nNOS inhibition with L-VNIO did not alter the cardiac biopterin profile.

In addition to the biopterin data, nitrite concentration, as an indicator of cardiac NO availability, showed that estrogen accounted for 21% of the total variance in tissue nitrite levels [Estrogen: $F(1,25) = 7.35$, $P = 0.012$], while L-VNIO did not change the cardiac concentrations of nitrite and hence, NO (Figure 5).

To determine whether estrogen or L-VNIO influences the cardiac NOS isoforms, we examined cardiac nNOS and eNOS expression. nNOS expression was increased 1.3-fold in the homogenates from OVX rats compared to estrogen-intact rats [Estrogen: $F(1,8) = 56.27$, $P < 0.005$] (Figure 6). The protein levels of eNOS were similar between OVX and intact littermates (Figure 6) as was the ratio of phosphorylated eNOS to total eNOS between the groups.

Discussion

The primary finding of the current study is that in the ovariectomized mRen2.Lewis rats, a model that emulates the cardiovascular phenotype in women following ovarian hormone loss, selective nNOS inhibition with L-VNIO attenuated cardiac superoxide production and limited cardiac remodeling, leading to improvements in diastolic function. As in previous reports,[23] diastolic function was worsened by removal of the ovaries. In the absence of estrogen, left ventricular relaxation was impaired while filling pressures tended to increase. These effects were coupled with myocardial structural alterations indicated by an increase in LV relative wall thickness (RWT) as well as increased cardiac collagen deposition. Four weeks of targeted nNOS inhibition attenuated the diastolic dysfunction phenotype of the ovariectomized mRen2.Lewis rats as revealed by echocardiographic-derived measures of myocardial relaxation and ventricular compliance. These functional changes were accompanied by reverse LV remodeling, as L-VNIO limited cardiac hypertrophy and perivascular collagen deposition in OVX-mRen2.Lewis rats. Importantly, these data are the first to show in the heart that OVX-elicited potentiation in ROS are abrogated by the nNOS inhibitor L-VNIO. These effects within the heart of the ovariectomized mRen2.Lewis appear to be due to diminished or oxidized BH4, the necessary cofactor for NOS activity, with concomitant increases in uncoupled nNOS and/or a reduction in NO production.

The adverse structural remodeling of the myocardium, indicated by increases in wall thickness, LV mass, and perivascular collagen, that contributes to the lusitropic dysfunction in the OVX-mRen2.Lewis rat appears to be rooted at the level of extracellular matrix. Several studies showed that estrogen loss is accompanied by increases in tissue collagen deposition which may in part be a consequence of increased cardiac Ang II tissue content or activity in this model.[23] Since serum levels of aldosterone are increased in ovariectomized mRen2.Lewis hypertensive rats,[23] this may contribute to collagen deposition within the heart. Other studies have implicated aldosterone as a potent profibrotic factor[32–34] and in previous reports in mRen2.Lewis rats,[25] L-VNIO treatment was associated with a decrease in serum aldosterone to levels found in non-ovariectomized rats.[26] It is plausible that the loss of estrogen accounts for the increased deposition, given that estrogen has been shown to regulate collagen turnover and fibroblast proliferation.[35,36] Certainly, the exacerbated hypertension in the estrogen-deplete mRen2.Lewis rats could contribute to extracellular matrix remodeling and diastolic dysfunction.

Importantly, L-VNIO offered a degree of cardioprotection among OVX-mRen2.Lewis rats that mitigated the diastolic dysfunction and attenuated LV remodeling. Since there were no overt changes in blood pressure in sham-operated rats at the end of the 4 wk of treatment,

the action of LVNIO appears to be directed to the myocardium rather than the peripheral vasculature. Indeed, diastolic functional derangements have been reported in isolated cardiomyocytes from hypertensive mice.[37] Moreover, L-VNIO treatment in our sham-operated (estrogen-intact) rats improved myocardial relaxation and reduced wall thicknesses, perivascular fibrosis, and ROS generation in the absence of changes in systolic blood pressure. In a recent report by Silberman at al.,[37] hypertensive mice given either hydralazine or BH4 experienced equivalent blood pressure reductions while improvements in diastolic function were detectable only in the BH4-treated mice. Taken together with our findings, these data implicate a direct role of cardiac NOS in the preservation of cardiac structure and diastolic function. Our data corroborate clinical and experimental studies which show cardiac functional improvements associated with decreased oxidative stress following blockade of the renin angiotensin system that are independent of blood pressure.[38–40]

The loss of the estrogenic stimulus on BH4 synthesis may uncouple nNOS shifting it to a maladaptive ROS generating state. In the ovariectomized mRen2.Lewis hypertensive rat, a discoordinate regulation of renal NOS isoforms was evident with reduced renal cortical mRNA and protein levels of eNOS while renal cortical nNOS mRNA and protein were increased.[26] In this situation, just as in our current study, nNOS is presumed to transition from catalyzing NO formation to generating superoxide.[41,42] While the precise mechanism for this conversion of nNOS is not clear, it may reflect estrogen sensitive regulation of guanosine triphosphate cyclohydrolase I (GTPCH), the rate limiting enzyme of BH4 synthesis.[43] Thus, in the absence of estrogen, the nNOS cofactor, BH4, may be oxidized or decreased overall leading to an increase in ROS at the biological expense of reduced NO. White and colleagues[44] emphasized the importance of age-related decreases in requisite components of NOS activity while demonstrating that nNOS specifically is an estrogen target in coronary vessels that can lead to detrimental or beneficial effects depending upon the surrounding milieu that determines the coupling state of the enzyme. In a coupled state, NOS is considered positive in that it generates NO. Alternatively, in situations where NOS becomes uncoupled, NOS activity can be detrimental by generating reactive oxygen species.

This idea of “uncoupling” is a rather novel phenomenon, which was first demonstrated in the heart and vascular beds predominantly related to eNOS.[45,46] More recently, it has been shown that nNOS uncoupling in the heart may regulate cardiac function.[47–49] Specifically, nNOS stimulates cardiac O_2^- production, modulates cardiac nitroso-redox balance, and stimulates development of diastolic dysfunction.[37] L-VNIO appears to have targeted this pathway as chronic administration of the inhibitor reduced the increase in ROS production while improving diastolic function following oophorectomy. According to Babu and Griffith,[50] L-VNIO is a potent, mechanism-based inhibitor blocking the heme cofactor of NOS which also shows a marked selectivity for nNOS. Typically, in the presence of NADPH and O_2, L-VNIO irreversibly inactivates nNOS through a Ca^{2+}/calmodulin-dependent effect. In the absence of BH4, inhibition of nNOS activity by L-VNIO is increased.[50] It is plausible that estrogen depletion and the subsequent BH4 reduction may have augmented the inhibitory capacity of L-VNIO on nNOS.[50] Taken together, these findings support the notion that estrogen has a regulatory role in the maintenance of cardiac structure and diastolic function in part through its modulation of myocardial NO production or by direct attenuation of the profibrotic actions of reactive oxygen species.

The present study has a few limitations. First, the pharmacological specificity of L-VNIO for nNOS as opposed to the other NOS isoforms is unconfirmed under the existing physiologic setting. In order to adequately address the precise contribution of nNOS blockade to alterations in NOS activity and to improvements in cardiovascular endpoints, parallel studies using nonspecific and specific-inhibitors of the other NOS’s would be

needed. While this is beyond the scope of our current study, several *ex vivo* cardiomyocyte studies performed by others do indeed show that L-VNIO is specific for nNOS. The initial study by Babu et al.[50] found the K_i of L-VNIO for nNOS to be 0.1 μM compared to values at least 100-times higher in eNOS (12 μM) and iNOS (60 μM). Another study utilizing isolated myocytes from wild-type and selective nNOS knockout mice show that L-VNIO-treated cells of wild-type mice have the same relaxation potential as that of cells rendered from knockout mice.[51] Elaborating upon their previous work, Casadei's group also showed that L-VNIO-treated cardiomyocytes from wild-type mice increase the sarcoplasmic reticulum Ca^{2+} load to a similar degree as myocytes isolated from nNOS knockout mice.[52] Therefore, taken together with the increased expression of nNOS in hearts from OVX-mRen2.Lewis rats and the abrogation of cardiac ROS production after administration of L-VNIO, suggests that the *in vivo* administration of L-VNIO conferred specificity for nNOS rather than eNOS.

Second, the physiologic perturbations from abrupt (via surgical manipulation) ovarian hormone loss in adult rodents are not analogous to that which occurs in middle-aged women following natural menopause. While artificial or surgical menopause represents less than 13% of women (see the web site http://www.menopause.org), reports have also linked premenopausal oophorectomy with unfavorable health consequences including increased cardiovascular risk.[53,54] As in humans, the mRen2.Lewis female rodent shows accelerated increases in blood pressure and left ventricular hypertrophy following ovarian hormone depletion. This strain, therefore, provides a unique model to study the role of ovarian hormones, independent of age-related cardiovascular changes, in the pathogenesis of diastolic heart disease in a 'high risk' population.

Conclusion

In summary, we show that estrogen depletion, due to the removal of the ovaries, in mRen2.Lewis female rats exacerbates diastolic dysfunction while invoking functionally diminished myocardial relaxation and altered cardiac pathology including increased LV relative wall thickness and collagen deposition. These detrimental effects were significantly attenuated following administration of a selective nNOS inhibitor, which we propose is due to the ability of L-VNIO to mitigate ROS generation.

Acknowledgments

The authors wish to thank Marina Lin, MS for her technical contributions and Timothy T. Houle, PhD for his statistical expertise.

Funding/support: The work described here was supported in part by grants from the National Institute of Health R01-AG033727-01 (LG), KO8-AG026764-05 Paul Beeson award (LG), NIH National Institute of Health HL058091 (DBK-S), R01 GM077352 (AFC), HL-56973 (MCC), and American Heart Association Grant-in-Aid 0855601GH (AFC).

References

1. Lloyd-Jones D, Adams R, Carnethon M, et al. Heart Disease and Stroke Statistics--2009 Update. A Report From the American Heart Association Statistics Committee and Stroke Statistics Subcommittee. Circulation. 2009; 119:e21–181. [PubMed: 19075105]
2. Owan TE, Hodge DO, Herges RM, Jacobsen SJ, Roger VL, Redfield MM. Trends in prevalence and outcome of heart failure with preserved ejection fraction. N Engl J Med. 2006; 355:251–9. [PubMed: 16855265]
3. Roger VL, Weston SA, Redfield MM, et al. Trends in heart failure incidence and survival in a community-based population. JAMA. 2004; 292:344–50. [PubMed: 15265849]

4. Masoudi FA, Havranek EP, Smith G, et al. Gender, age, and heart failure with preserved left ventricular systolic function. J Am Coll Cardiol. 2003; 41:217–23. [PubMed: 12535812]
5. Tsutsui H, Tsuchihashi-Makaya M, Kinugawa S, Goto D, Takeshita A. Clinical characteristics and outcome of hospitalized patients with heart failure in Japan. Circ J. 2006; 70(12):1617–23. [PubMed: 17127810]
6. Wong DT, Clark RA, Dundon BK, Philpott A, Molaee P, Shakib S. Caveat anicula! Beware of quiet little old ladies: demographic features, pharmacotherapy, readmissions and survival in a 10-year cohort of patients with heart failure and preserved systolic function. Med J Aust. 2010; 192:9–13. [PubMed: 20047541]
7. Levy D, Kenchaiah S, Larson MG, et al. Long-term trends in the incidence of and survival with heart failure. N Engl J Med. 2002; 347:1397–402. [PubMed: 12409541]
8. Rusinaru D, Mahjoub H, Goissen T, Massy Z, Peltier M, Tribouilloy C. Clinical features and prognosis of heart failure in women. A 5-year prospective study. Int J Cardiol. 2009; 133:327–35. [PubMed: 18457887]
9. Agabiti-Rosei E, Muiesan ML. Left ventricular hypertrophy and heart failure in women. J Hypertens Suppl. 2002; 20:S34–S38. [PubMed: 12183849]
10. Oberman A, Prineas RJ, Larson JC, LaCroix A, Lasser NL. Prevalence and determinants of electrocardiographic left ventricular hypertrophy among a multiethnic population of postmenopausal women (The Women's Health Initiative). Am J Cardiol. 2006; 97:512–9. [PubMed: 16461048]
11. Fak AS, Erenus M, Tezcan H, Caymaz O, Oktay S, Oktay A. Effects of a single dose of oral estrogen on left ventricular diastolic function in hypertensive postmenopausal women with diastolic dysfunction. Fertil Steril. 2000; 73:66–71. [PubMed: 10632414]
12. Rossouw JE, Anderson GL, Prentice RL, et al. Risks and benefits of estrogen plus progestin in healthy postmenopausal women: principal results From the Women's Health Initiative randomized controlled trial. JAMA. 2002; 288:321–33. [PubMed: 12117397]
13. Javeshghani D, Schiffrin EL, Sairam MR, Touyz RM. Potentiation of vascular oxidative stress and nitric oxide-mediated endothelial dysfunction by high-fat diet in a mouse model of estrogen deficiency and hyperandrogenemia. J Am Soc Hypertens. 2009; 3:295–305. [PubMed: 20409973]
14. Maric C, Xu Q, Sandberg K, Hinojosa-Laborde C. Age-related renal disease in female Dahl salt-sensitive rats is attenuated with 17 beta-estradiol supplementation by modulating nitric oxide synthase expression. Gend Med. 2008; 5:147–59. [PubMed: 18573482]
15. Santos RL, Abreu GR, Bissoli NS, Moyses MR. Endothelial mediators of 17 beta-estradiol-induced coronary vasodilation in the isolated rat heart. Braz J Med Biol Res. 2004; 37:569–75. [PubMed: 15064820]
16. Staessen J, Bulpitt CJ, Fagard R, Lijnen P, Amery A. The influence of menopause on blood pressure. J Hum Hypertens. 1989; 3:427–33. [PubMed: 2607517]
17. Raij L. Nitric oxide in the pathogenesis of cardiac disease. J Clin Hypertens (Greenwich). 2006; 8(12 Suppl 4):30–9. [PubMed: 17170604]
18. Garcia-Duran M, de FT, az-Recasens J, et al. Estrogen stimulates neuronal nitric oxide synthase protein expression in human neutrophils. Circ Res. 1999; 85:1020–6. [PubMed: 10571532]
19. Molero L, Garcia-Duran M, Diaz-Recasens J, Rico L, Casado S, Lopez-Farre A. Expression of estrogen receptor subtypes and neuronal nitric oxide synthase in neutrophils from women and men: regulation by estrogen. Cardiovasc Res. 2002; 56:43–51. [PubMed: 12237165]
20. Qian X, Jin L, Lloyd RV. Estrogen downregulates neuronal nitric oxide synthase in rat anterior pituitary cells and GH3 tumors. Endocrine. 1999; 11:123–30. [PubMed: 10709758]
21. Salhab WA, Shaul PW, Cox BE, Rosenfeld CR. Regulation of types I and III NOS in ovine uterine arteries by daily and acute estrogen exposure. Am J Physiol Heart Circ Physiol. 2000; 278:H2134–H2142. [PubMed: 10843913]
22. Nuedling S, Karas RH, Mendelsohn ME, et al. Activation of estrogen receptor beta is a prerequisite for estrogen-dependent upregulation of nitric oxide synthases in neonatal rat cardiac myocytes. FEBS Lett. 2001; 502:103–8. [PubMed: 11583108]

23. Groban L, Yamaleyeva LM, Westwood BM, et al. Progressive diastolic dysfunction in the female mRen(2). Lewis rat: influence of salt and ovarian hormones. J Gerontol A Biol Sci Med Sci. 2008; 63:3–11. [PubMed: 18245755]
24. Ferrario CM, Jessup J, Chappell MC, et al. Effect of angiotensin-converting enzyme inhibition and angiotensin II receptor blockers on cardiac angiotensin-converting enzyme 2. Circulation. 2005; 111:2605–10. [PubMed: 15897343]
25. Chappell MC, Westwood BM, Yamaleyeva LM. Differential effects of sex steroids in young and aged female mRen2. Lewis rats: a model of estrogen and salt-sensitive hypertension. Gend Med. 2008; 5(Suppl A):S65–S75. [PubMed: 18395684]
26. Yamaleyeva LM, Gallagher PE, Vinsant S, Chappell MC. Discoordinate regulation of renal nitric oxide synthase isoforms in ovariectomized mRen2. Lewis rats. Am J Physiol Regul Integr Comp Physiol. 2007; 292:R819–R826. [PubMed: 17023669]
27. Jessup JA, Westwood BM, Chappell MC, Groban L. Dual ACE-inhibition and AT1 receptor antagonism improves ventricular lusitropy without affecting cardiac fibrosis in the congenic mRen2. Lewis rat. Ther Adv Cardiovasc Dis. 2009; 3:245–57. [PubMed: 19531557]
28. Zheng JS, Yang XQ, Lookingland KJ, et al. Gene transfer of human guanosine 5′-triphosphate cyclohydrolase I restores vascular tetrahydrobiopterin level and endothelial function in low renin hypertension. Circulation. 2003; 108:1238–45. [PubMed: 12925450]
29. Bryan NS, Fernandez BO, Bauer SM, et al. Nitrite is a signaling molecule and regulator of gene expression in mammalian tissues. Nat Chem Biol. 2005; 1:290–7. [PubMed: 16408059]
30. Lam KK, Lee YM, Hsiao G, Chen SY, Yen MH. Estrogen therapy replenishes vascular tetrahydrobiopterin and reduces oxidative stress in ovariectomized rats. Menopause. 2006; 13:294–302. [PubMed: 16645543]
31. Shi W, Meininger CJ, Haynes TE, Hatakeyama K, Wu G. Regulation of tetrahydrobiopterin synthesis and bioavailability in endothelial cells. Cell Biochem Biophys. 2004; 41:415–34. [PubMed: 15509890]
32. Sam F, Duhaney TA, Sato K, et al. Adiponectin deficiency, diastolic dysfunction, and diastolic heart failure. Endocrinology. 2010; 151:322–31. [PubMed: 19850745]
33. Shieh FK, Kotlyar E, Sam F. Aldosterone and cardiovascular remodelling: focus on myocardial failure. J Renin Angiotensin Aldosterone Syst. 2004; 5:3–13. [PubMed: 15136967]
34. Tsybouleva N, Zhang L, Chen S, et al. Aldosterone, through novel signaling proteins, is a fundamental molecular bridge between the genetic defect and the cardiac phenotype of hypertrophic cardiomyopathy. Circulation. 2004; 109:1284–91. [PubMed: 14993121]
35. Dubey RK, Gillespie DG, Jackson EK, Keller PJ. 17Beta-estradiol, its metabolites, and progesterone inhibit cardiac fibroblast growth. Hypertension. 1998; 31(1 Pt 2):522–8. [PubMed: 9453356]
36. Xu Y, Arenas IA, Armstrong SJ, Davidge ST. Estrogen modulation of left ventricular remodeling in the aged heart. Cardiovasc Res. 2003; 57:388–94. [PubMed: 12566111]
37. Silberman GA, Fan TH, Liu H, et al. Uncoupled cardiac nitric oxide synthase mediates diastolic dysfunction. Circulation. 2010; 121:519–28. [PubMed: 20083682]
38. Futai R, Ito T, Kawanishi Y, Terasaki F, Kitaura Y. Olmesartan ameliorates myocardial function independent of blood pressure control in patients with mild-to-moderate hypertension. Heart Vessels. 2009; 24:294–300. [PubMed: 19626403]
39. Nishio M, Sakata Y, Mano T, et al. Therapeutic effects of angiotensin II type 1 receptor blocker at an advanced stage of hypertensive diastolic heart failure. J Hypertens. 2007; 25:455–61. [PubMed: 17211254]
40. Yoshida J, Yamamoto K, Mano T, et al. AT1 receptor blocker added to ACE inhibitor provides benefits at advanced stage of hypertensive diastolic heart failure. Hypertension. 2004; 43:686–91. [PubMed: 14757777]
41. Alderton WK, Cooper CE, Knowles RG. Nitric oxide synthases: structure, function and inhibition. Biochem J. 2001; 357:593–615. [PubMed: 11463332]
42. Gorren AC, Schrammel A, Riethmuller C, et al. Nitric oxide-induced autoinhibition of neuronal nitric oxide synthase in the presence of the autoxidation-resistant pteridine 5-methyltetrahydrobiopterin. Biochem J. 2000; 347:475–84. [PubMed: 10749677]

43. Serova LI, Maharjan S, Sabban EL. Estrogen modifies stress response of catecholamine biosynthetic enzyme genes and cardiovascular system in ovariectomized female rats. Neuroscience. 2005; 132:249–59. [PubMed: 15802180]
44. White RE, Han G, Dimitropoulou C, et al. Estrogen-induced contraction of coronary arteries is mediated by superoxide generated in vascular smooth muscle. Am J Physiol Heart Circ Physiol. 2005; 289:H1468–H1475. [PubMed: 16162867]
45. Moens AL, Takimoto E, Tocchetti CG, et al. Reversal of cardiac hypertrophy and fibrosis from pressure overload by tetrahydrobiopterin: efficacy of recoupling nitric oxide synthase as a therapeutic strategy. Circulation. 2008; 117:2626–36. [PubMed: 18474817]
46. Takimoto E, Champion HC, Li M, et al. Oxidant stress from nitric oxide synthase-3 uncoupling stimulates cardiac pathologic remodeling from chronic pressure load. J Clin Invest. 2005; 115:1221–31. [PubMed: 15841206]
47. Moens AL, Leyton-Mange JS, Niu X, et al. Adverse ventricular remodeling and exacerbated NOS uncoupling from pressure-overload in mice lacking the beta3-adrenoreceptor. J Mol Cell Cardiol. 2009; 47:576–85. [PubMed: 19766235]
48. Umar S, van der Laarse A. Nitric oxide and nitric oxide synthase isoforms in the normal, hypertrophic, and failing heart. Mol Cell Biochem. 2010; 333:191–201. [PubMed: 19618122]
49. Zhang GX, Kimura S, Murao K, Shimizu J, Matsuyoshi H, Takaki M. Role of neuronal NO synthase in regulating vascular superoxide levels and mitogen-activated protein kinase phosphorylation. Cardiovasc Res. 2009; 81:389–99. [PubMed: 18987049]
50. Babu BR, Griffith OW. N5-(1-Imino-3-butenyl)-L-ornithine. A neuronal isoform selective mechanism-based inactivator of nitric oxide synthase. J Biol Chem. 1998; 273:8882–9. [PubMed: 9535869]
51. Ashley EA, Sears CE, Bryant SM, Watkins HC, Casadei B. Cardiac nitric oxide synthase 1 regulates basal and beta-adrenergic contractility in murine ventricular myocytes. Circulation. 2002; 105:3011–6. [PubMed: 12081996]
52. Sears CE, Bryant SM, Ashley EA, et al. Cardiac neuronal nitric oxide synthase isoform regulates myocardial contraction and calcium handling. Circ Res. 2003; 92:e52–9. [PubMed: 12623875]
53. Lobo RA. Surgical menopause and cardiovascular risks. Menopause. 2007; 14:562–6. [PubMed: 17476145]
54. Shuster LT, Gostout BS, Grossardt BR, Rocca WA. Prophylactic oophorectomy in premenopausal women and long-term health. Menopause Int. 2008; 14:111–6. [PubMed: 18714076]

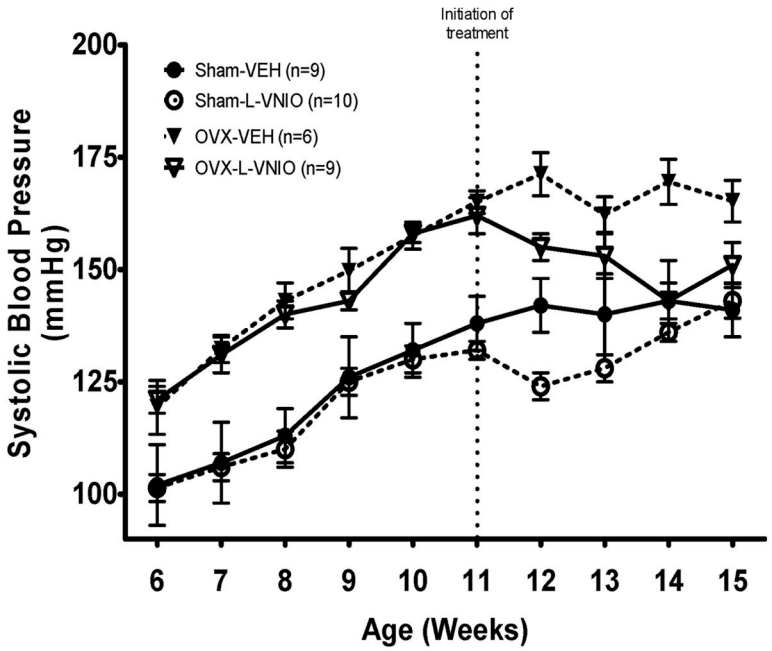

Figure 1.
Tail-cuff systolic blood pressure in sham-operated or OVX conscious female mRen2.Lewis rats treated with L-VNIO or saline vehicle for 4 weeks. Values are means ± SEM.

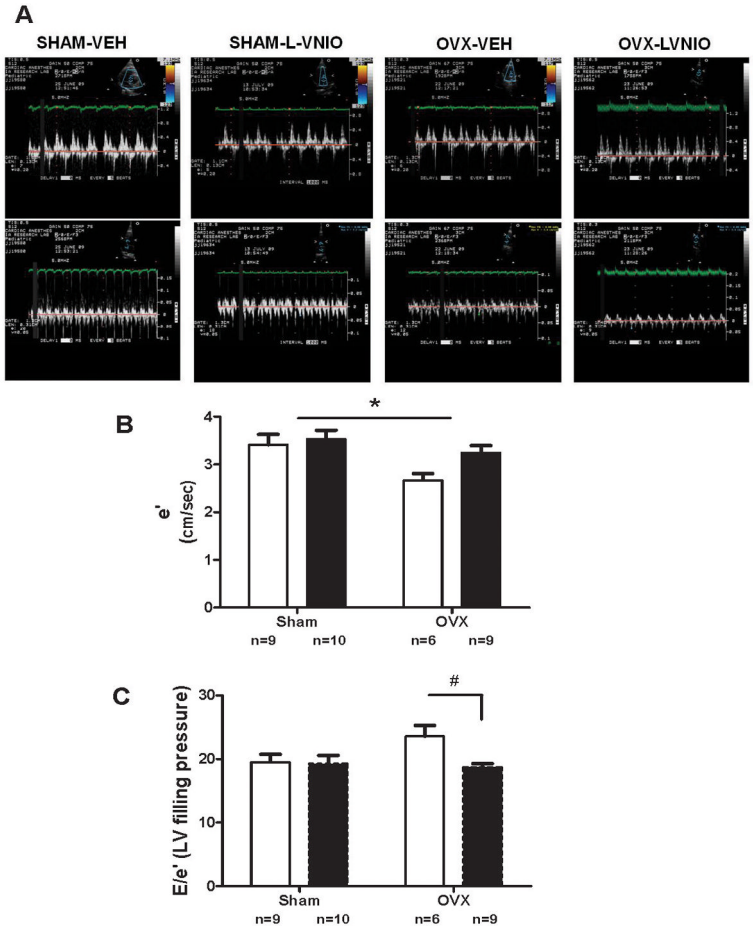

Figure 2.

A. Representative tissue Doppler image of intact or OVX mRen2.Lewis female receiving either vehicle or combination. E = early transmitral filling velocity; A = late transmitral filling velocity; e′ = early mitral annular descent (septal) velocity. B. Early mitral annular velocity (e′). Open bars are vehicle treated, while filled bars received L-VNIO. Data represent mean ± SEM; * P < 0.01 (Estrogen effect). C. Early transmitral filling velocity – to – mitral annular velocity ratio (E/e′). Data represent mean ± SEM; * P < 0.05 (L-VNIO effect).

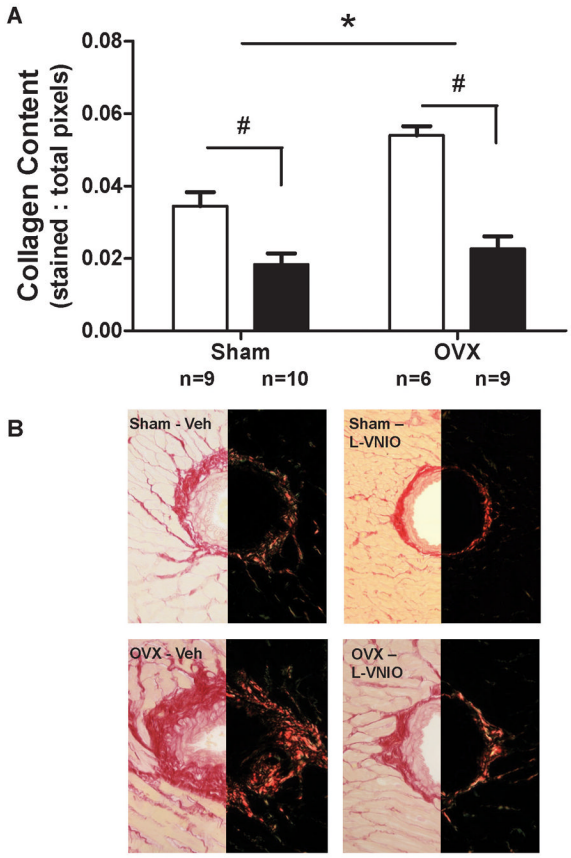

Figure 3.

Quantification and representative picrosirius red staining of perivascular collagen in the hearts of sham-operated, ovariectomized (OVX), and rats given the nNOS inhibitor (L-VNIO). Open bars are vehicle treated, while filled bars received L-VNIO. Data represent mean ± SEM; * P = 0.0005 (Estrogen effect), # P < 0.0001 (L-VNIO effect).

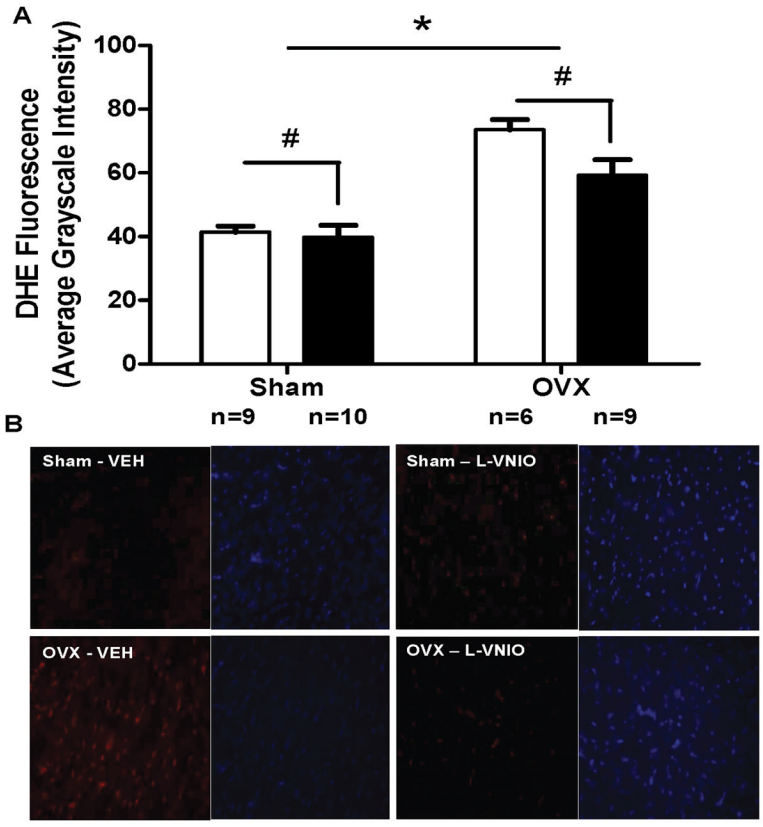

Figure 4.

Quantification and representative images illustrating the effect of L-VNIO on cardiac levels of fluorescent 2-hydroxyethidium from dihydroethidium (DHE) staining in estrogen intact (sham) or OVX. Open bars represent vehicle treated rats, while filled bars received L-VNIO. Fluorescent images are shown at 400× magnification. Data represent mean ± SEM; * $P < 0.0001$ (Estrogen effect), # $P = 0.0326$ (L-VNIO effect).

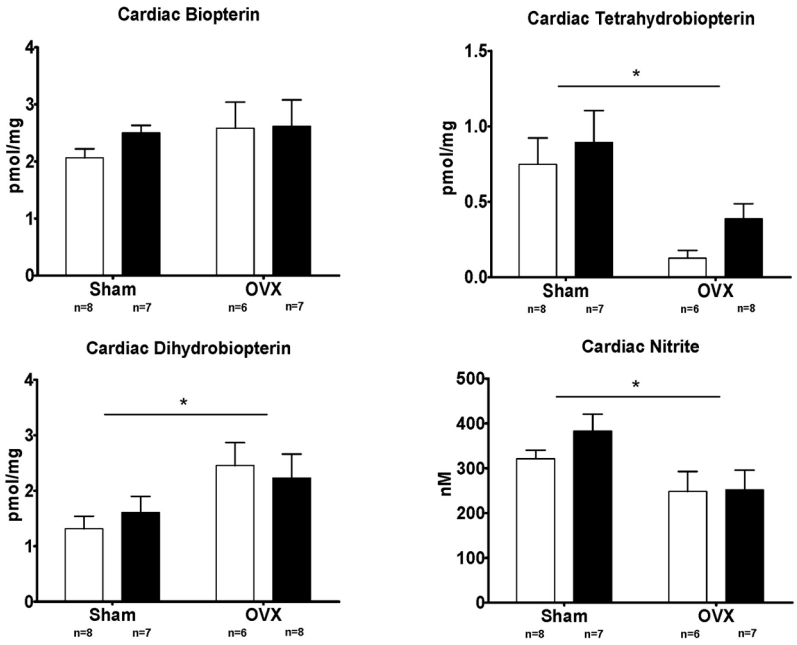

Figure 5.

Cardiac concentrations of biopterin, BH2, BH4, and nitrite. Open bars are vehicle treated, while filled bars received L-VNIO. Data represent mean ± SEM; * $P < 0.01$ (Estrogen effect).

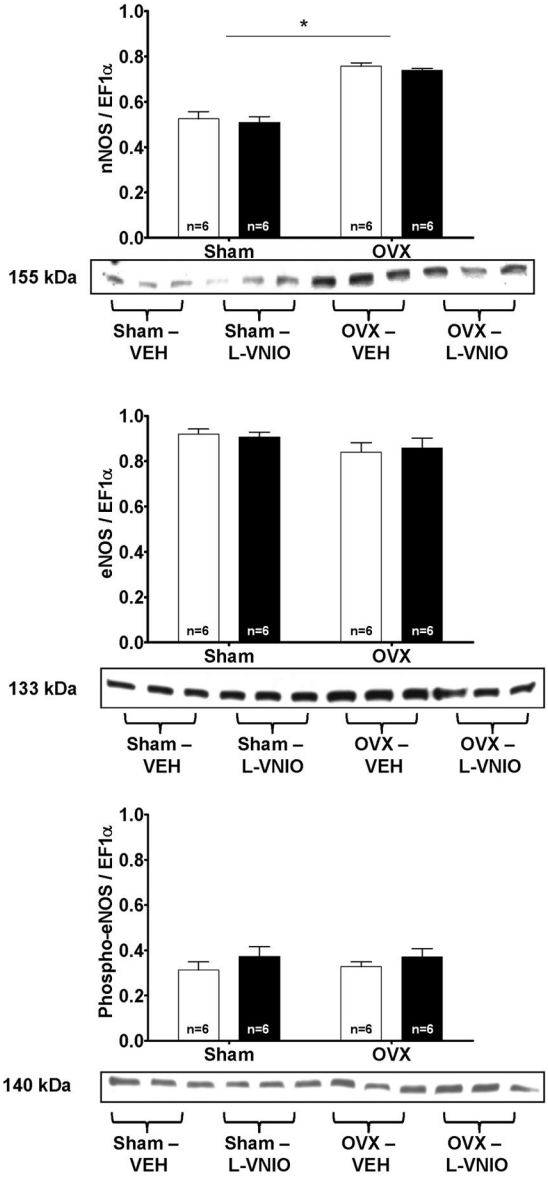

Figure 6.

Values are means ± SEM of cardiac nNOS, total eNOS, and phosphorylated eNOS protein expression in sham-operated or OVX rats treated with VEH or L-VNIO treated rats. Open bars are vehicle treated, while filled bars received L-VNIO. * $P < 0.005$ (Estrogen effect).

Table 1

Body and Heart Weight Values

	Sham		OVX		P value		
	Vehicle	**L-VNIO**	**Vehicle**	**L-VNIO**	**Estrogen**	**L-VNIO**	**Interaction**
Body weight, *g*	240 ± 9	238 ± 5	276 ± 13	280 ± 7	***0.0001***	0.781	0.533
Heart weight, *mg*	818 ± 0.02	822 ± 0.02	925 ± 0.01	932 ± 0.01	***0.002***	0.873	0.960
Heart weight/Body weight, *mg/g*	3.42 ± 0.08	3.47 ± 0.09	3.35 ± 0.12	3.33 ± .09	0.461	0.918	0.773

Data are expressed as mean ± SEM.

Menopause. Author manuscript; available in PMC 2012 June 1.

Table 2

Echocardiographic Indices of Systolic and Diastolic Function

	Sham		OVX		P value		
	Vehicle	**L-VNIO**	**Vehicle**	**L-VNIO**	**Estrogen**	**L-VNIO**	**Interaction**
Heart Rate, *bpm*	250 ± 9	244 ± 5	206 ± 13	228 ± 7	0.156	0.357	0.753
LVEDD, *cm*	0.68 ± 0.02	0.68 ± 0.02	0.68 ± 0.01	0.69 ± 0.01	0.757	0.752	0.763
LVESD, *cm*	0.37 ± 0.02	0.37 ± 0.02	0.37 ± 0.02	0.40 ± 0.01	0.518	0.271	0.350
RWT	1.07 ± 0.08	1.28 ± 0.09	1.02 ± 0.11	1.16 ± 0.09	***0.002***	***0.004***	0.211
%FS	46 ± 2	46 ± 1	46 ± 2	43 ± 2	0.562	0.365	0.499
E_{max}, cm/sec	64 ± 2	66 ± 3	61 ± 3	61 ± 3	0.147	0.909	0.693
E_{dec}slope, cm/sec^2	11 ± 1	13 ± 1	10 ± 1	11 ± 1	***0.033***	0.128	0.875
A_{max}, cm/sec	42 ± 3	38 ± 2	42 ± 3	41 ± 2	0.637	0.357	0.652
E/A	1.57 ± 0.09	1.76 ± 0.13	1.47 ± 0.12	1.49 ± 0.08	***0.085***	0.348	0.461
e′, cm/sec	3.40 ± 0.22	3.52 ± 0.19	2.66 ± 0.14	3.24 ± 0.15	***0.011***	***0.076***	0.235
E/e′	19.5 ± 1.23	19.2 ± 1.32	23.6 ± 1.7	18.7 ± 0.55	0.162	***0.048***	0.077
a′, cm/sec	3.20 ± 0.09	2.82 ± 0.16	2.75 ± 0.31	2.95 ± 0.28	0.451	0.718	0.191
e′/a′	3.20 ± 0.09	2.82 ± 0.16	2.75 ± 0.31	2.95 ± 0.28	0.617	***0.038***	0.492

Data are expressed as mean ± SEM. LVEDD = left ventricular end-diastolic dimension; LVESD = left ventricular end-systolic dimension; RWT = relative wall thickness; %FS = percent fractional shortening; E_{max} = maximum early transmitral filling velocity; E_{dec}slope = early-filling deceleration slope; A_{max} = maximum late transmitral filling velocity; E/A = early-to-late transmitral filling ratio; e′ = early mitral annular velocity; E/e′ = early transmitral filling velocity-to-mitral annular velocity; a′ = late mitral annular velocity; e′/a′ = early-to-late mitral annular ratio.